

## **FINITE LENGTH OMNI-DIRECTIONAL CYLINDRICAL SPATIAL FILTERS**

**A. E. Farahat and K. F. A. Hussein**

Microwave Engineering Department  
Electronics Research Institute  
Dokki, Cairo, Egypt

**N. M. El-Minyawi**

Faculty of Engineering  
Ain Shams University  
Egypt

**Abstract**—A finite length cylindrical FSS is proposed as a spatial filter for both transmitting and receiving antennas. This filter has the advantage of not perturbing the omnidirectional property of the enclosed antenna. The proposed surface is constructed up as cylindrical array of rectangular conducting patches. The strips are arranged periodically in the  $\phi$ - and  $z$ -directions. The electric field integral equation (EFIE) approach is used for analyzing the characteristics of the proposed spatial filter. The Rao-Wilton-Glisson (RWG) basis functions are used for current expansion on the conducting strips. The mutual effects between the filter and the antenna can be accurately investigated. The effects of some dimensional parameters on the filter characteristics, such as, the axial and angular spacing between the array elements, the length and the radius of the cylindrical surface are studied over a wide frequency range. The oblique incidence of plane waves on such a cylindrical filter is studied with varying the direction of incidence. The performance of the proposed spatial filter is examined when operating with nearby antennas. The effects of such a filter on the input impedance, VSWR, and radiation pattern of an enclosed bowtie antenna are investigated over a wide frequency range.

## 1. INTRODUCTION

The frequency selective surface (FSS) is a useful filter for electromagnetic radiation ranging from microwave to optical frequencies [1]. At microwave frequencies, the surface can be composed of an array of conducting patches or apertures in a conducting sheet. When the FSS is constructed from a planar array of elements, an incident spectrum of plane waves filtered by the surface will exhibit a bandpass or band-stop behavior, which is dependent upon the surface characteristics. In many FSS applications, the surface is constructed from non-planar curved or closed, finite array of elements, and may not be illuminated by a plane wave. A sub-reflector in a reflector antenna system is an example which is both non-planar and has spherical wave incidence [2].

Spatial filters are important for many applications such as in hybrid radomes [3], interference reduction in wireless environment [4], and for antennas as the dual reflector antenna proposed in [5, 6].

Determining the characteristics of a finite size planar frequency selective surface (FSS) is a difficult problem that has been addressed using approximate spectral domain techniques. When the surface becomes curved and of finite size, it turns out to be a formidable problem that can't be handled using the known techniques except for special surfaces with some approximations. Designing cylindrical spatial filter is important for omni-directional antennas. It is preferred to the planar spatial filters, as they will filter out radiation within their stop band in all the circumferential directions, whereas the planar FSS will filter out radiation only in a specified range of angles, in the direction where the FSS is put.

The planar FSS can be conveniently formulated by using a plane wave spectral representation for the scattered fields [7–9]. However, modeling the scattered fields from curved FSS is a difficult problem. Some results have been achieved when the surface conforms to a circular cylinder of finite axial length, such that fields can be expanded in terms of cylindrical wave functions [10–12]. As in the planar surface, currents and fields are represented by a superposition of Floquet harmonics. The harmonics (cylindrical waves) are found in the specific coordinate system and are the characteristic functions of the system. The scattered fields from the surface can then be obtained from the calculated currents. Since this technique assumes that the cylinder is infinite, it will not be able to handle finite cylinder or curved FSS.

The approximate locally planar technique (LPT) method can be used to determine the scattering from planar or curved FSS [13–15]. The LPT involves dividing the surface into a number of patches, each of which is assumed to be a segment of an infinite planar surface. The

surface current on each patch is assumed to be the same as the current induced on the center patch of a planar array which is tangential to the curved surface at the patch. The planar array problem is solved by the spectral Galerkin's method [8]. The scattered pattern from each of these patches is computed from the current induced on the patch. The superposition principle is invoked to obtain the scattering from the conformal array. Unfortunately, there are some limitations in the FSS geometries that can be studied by the LPT, as the LPT accuracy will deteriorate with increasing the curvature of the FSS. Also, at some incidence phase front curvature and or surface curvature, the LPT will no longer be a good approximation [14].

In the above methods, it is not feasible to study the mutual effects between the FSS and a nearby object as an antenna. In this case, a full wave numerical method of analysis must be employed. In this paper the electric field integral equation (EFIE) approach with triangular basis function [16, 17] is used for investigating the filtering characteristics of a free standing finite length FSS structure conformed to a cylindrical surface. This cylindrical FSS is utilized as a band stop spatial filter. The effect of the cylindrical spatial filter on the radiation characteristics of a bowtie antenna enclosed by such a surface is investigated.

## 2. EVALUATION OF THE SPATIAL FILTER RESPONSE

The EFIE approach with triangular basis functions [16, 17] is applied for analyzing the filtering characteristics of a free standing finite length cylindrical FSS. The EFIE technique has previously been applied for the analysis of the scattering from free standing finite planar structures [18]. Compared with other simulation approaches, the EFIE approach presents a number of advantages. For example, it gives flexibility to model structures of real size and of non-flat, arbitrarily shaped conducting structures. It enables us to study the filtering characteristics of FSS placed in the vicinity of an antenna, as well as the effect of the FSS on the antenna performance. Placing the antenna near the FSS violates its periodicity and, hence, violates the application of the ordinary spectral domain methods [7–9]. Beside all of the above it gives us high solution accuracy. In this work, an array of free standing rectangular strips is arranged on a cylindrical surface with its axis along the  $z$ -direction. Each strip is modeled using a surface model with 16 triangular patches as shown in Figure 1. The model of the proposed cylindrical FSS is shown in Figure 2.



**Figure 1.** Triangular patches model of the strip patch.

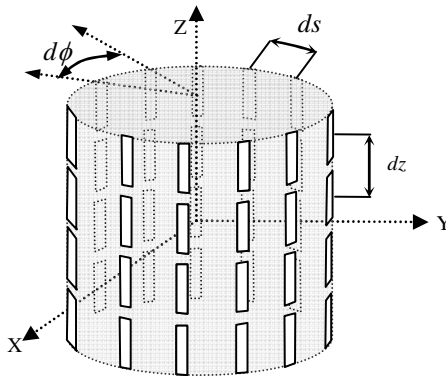


**Figure 2.** Free standing finite array of conducting strips conformed to a cylindrical surface.

### 2.1. Cylindrical Spatial Filter Response Due to Plane Wave Incidence

The frequency response of a cylindrical spatial filter is calculated due to an incident plane wave. The amplitude of the transmitted near field at the center point of the cylinder axis is divided by the amplitude of the incident plane wave to get a normalized frequency response,  $E_r$

$$E_r = \frac{|E_{transmitted}|}{|E_{incident}|} \quad (1)$$

The near field is calculated in a similar way as in [19], where the electric field components can be numerically calculated by discretizing the equation governing the relationship between the electric field and, the scalar and vector potentials,

$$\mathbf{E}(\mathbf{r}) = -j\omega\mathbf{A}(\mathbf{r}) - \nabla\Phi(\mathbf{r}) \quad (2)$$

where,  $\mathbf{A}(\mathbf{r})$  is the magnetic vector potential, and  $\Phi(\mathbf{r})$  is the electric scalar potential. These computations are enabled by discretizing the three-dimensional space of the problem into cubic cells. In this way,

the electric field components can be calculated as follows,

$$E_x|_{i,j,k} = -j\omega A_x|_{i,j,k} - \frac{1}{\Delta x} \left( \Phi|_{i+1,j,k} - \Phi|_{i-1,j,k} \right) \quad (3)$$

$$E_y|_{i,j,k} = -j\omega A_y|_{i,j,k} - \frac{1}{\Delta y} \left( \Phi|_{i,j+1,k} - \Phi|_{i,j-1,k} \right) \quad (4)$$

$$E_z|_{i,j,k} = -j\omega A_z|_{i,j,k} - \frac{1}{\Delta z} \left( \Phi|_{i,j,k+1} - \Phi|_{i,j,k-1} \right) \quad (5)$$

where  $i$ ,  $j$ , and  $k$ , are the indices of the vertices of the cubic cells in  $x$ ,  $y$ , and  $z$ -directions respectively.  $\Delta x$ ,  $\Delta y$ , and  $\Delta z$  are the cubic cell dimensions in  $x$ ,  $y$ , and  $z$ -directions respectively.

## 2.2. Performance Evaluation of a Spatial Filter Enclosing an Antenna

The Mutual effects between the cylindrical FSS and an enclosed antenna are investigated. The radiated field of the antenna is calculated in the presence and the absence of the cylindrical spatial filter. To ensure a fixed value for the input power, the radiated field is divided by the input power at each frequency. The antenna is assumed to be matched at  $300\Omega$ . The input power  $P_{in}$  is calculated as the sum of the accepted power,  $P_{acc}$ , and the reflected power,  $|\Gamma|^2 P_{in}$ , where  $\Gamma$  is the reflection coefficient,

$$P_{in} = P_{acc} + |\Gamma|^2 P_{in} \quad (6)$$

where,

$$P_{acc} = |V_{in}| |I_{in}| \cos \theta_p \quad (7)$$

$$\Gamma = \frac{Z_{in} - Z_o}{Z_{in} + Z_o} \quad (8)$$

$V_{in}$  and  $I_{in}$  are the voltage across and calculated input current at the antenna feed [20].  $\theta_p$  is the phase angle between  $V_{in}$  and  $I_{in}$ .  $Z_o$  is the transmission line impedance. The normalized radiated field is then given as,

$$E_{normalized} = \frac{E_{radiated}}{\sqrt{\eta P_{in}}} \quad (9)$$

where  $\eta$  is the free space intrinsic impedance. Now the cylindrical filter performance in the presence of the antenna is characterized by dividing the normalized radiated field in the presence of the cylindrical spatial filter by the normalized radiated field in its absence,

$$E_r = \frac{|E_{normalized(FSS\ present)}|}{|E_{normalized(FSS\ absent)}|} \quad (10)$$

In order to obtain the relation between the filter response and the design parameters, such as, the strip length and width, distances between strips in the longitudinal and circumferential direction, the radius and length of the cylindrical FSS, the effects of these parameters are investigated over a wide frequency range. The effect of the angle of incidence on the filter response is also investigated. The mutual effects between the FSS and an enclosed bowtie antenna are studied.

### 3. RESULTS AND DISCUSSIONS

This section is divided into two parts. In the first part, the cylindrical FSS is exposed to an incident plane wave incident normally on the axis of the cylindrical surface with the electric field in the direction of the cylinder axis. The total field at the mid point of the axis is calculated over the frequency range 5–15 GHz. The field calculated at the center point of the cylindrical cavity is divided by the amplitude of the incident plane wave to obtain the frequency response of the FSS. The frequency response is investigated when varying the interelement spacing, radius, and length of the cylinder. The filter response is also studied for different angles of incidence. The size of the array is expressed as  $N \times M$ , where  $N$  and  $M$  indicate the number of elements in the  $\phi$  and  $z$ -directions, respectively. The cylinder axis is always aligned with the  $z$ -axis unless otherwise is stated.

The second part discusses the frequency behavior of a linearly polarized bowtie antenna when placed inside the cylindrical spatial filter. The frequency behavior is studied when the bowtie antenna is used as a transmitter and when used as a receiver as well. For a transmitting bowtie antenna enclosed by the cylindrical spatial filter, the normalized radiated field in the presence of the filter is compared to the normalized radiated field in the absence of the filter. When the bowtie is used as a receiver, a plane wave is assumed normally incident on the cylindrical spatial filter, and the induced voltage across the gap at the center of the bowtie is calculated. The effect of the FSS on the input impedance and, hence, the VSWR of the antenna is investigated over the frequency range 5–15 GHz. Also, the effect of the spatial filter on the radiation pattern of the bowtie antenna is illustrated at different frequencies.

#### 3.1.

##### *3.1.1. Frequency Response of the Cylindrical Spatial Filter*

The frequency response of a free standing cylindrical spatial filter similar to that shown in Figure 2, composed of 10 elements in  $\phi$ -

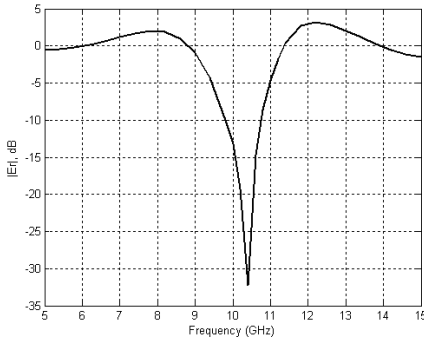


**Figure 3.** Frequency response of a  $10 \times 10$  cylindrical FSS with  $r = 1.9$  cm,  $d\phi = 36^\circ$ , and  $dz = 2.4$  cm, strip dimensions are  $1.5 \times 0.045$  cm, due to an incident plane wave propagating in the  $x$ -direction with vertical polarization, at the midpoint of the axis of the cylinder.

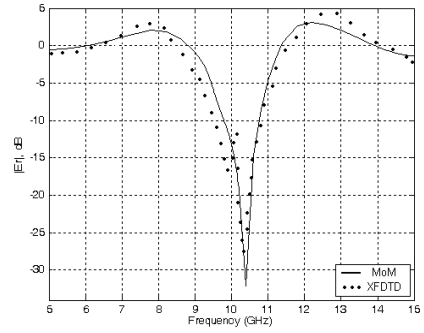


**Figure 4.** Frequency response of a  $10 \times 10$  cylindrical FSS with  $r = 1.9$  cm,  $d\phi = 36^\circ$ , and  $dz = 2.4$  cm, strip dimensions are  $1.5 \times 0.045$  cm due to an incident  $x$ -directed plane wave with vertical polarization, compared to the same frequency response obtained with FDTD.

direction and 10 elements in the  $z$ -direction is investigated. Each strip has a length  $L = 1.5$  cm and width  $W = 0.045$  cm. The spacing between the array elements in the  $z$ -direction is  $dz = 2.4$  cm. The horizontal angular spacing between any two adjacent strips is  $d\phi = 36^\circ$ . The radius of the cylinder is 1.9 cm. A plane wave is assumed incident on the structure, propagating in the  $x$ -direction with the electric field in the  $z$ -direction. The normalized spatial filter response is obtained in the frequency range 5–15 GHz. As shown in Figure 3, the cylindrical FSS exhibits a stop band filter response. It can be deduced from Figure 3 that the center frequency of the band stop filter occurs when the strip length is nearly half the wave length of the incident plane wave. The effects of the different design parameters on the filter response are investigated in the following sections.

In Figure 4, the frequency response of the same cylindrical spatial filter is obtained using the finite difference time domain (FDTD) commercial software XFDTD and compared to that obtained using the MoM showing good agreement.

### 3.1.2. Effect of Strip Dimensions on the Filter Response

The effect of the strip length constructing the cylindrical spatial filter on its frequency response is studied for lengths 1.3, 1.5, 1.7, and 1.9 cm.

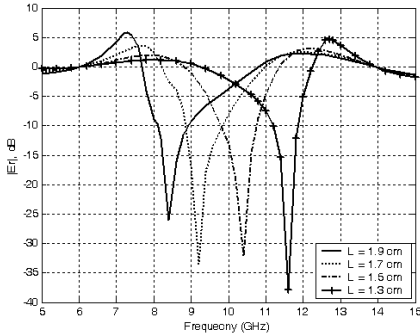


**Figure 5.** Frequency response of a  $10 \times 10$  cylindrical FSS,  $r = 1.9$  cm,  $dz = 2.4$  cm,  $d\phi = 36^\circ$ , and strip width  $W = 0.045$  cm, due to a vertical polarized normally incident plane wave, at the mid-point of the axis of the cylinder, for different strip lengths.

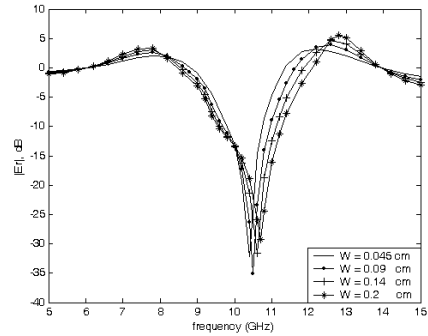


**Figure 6.** Frequency response of a  $10 \times 10$  cylindrical FSS,  $r = 1.9$  cm,  $dz = 2.4$  cm,  $d\phi = 36^\circ$ , and strip length  $L = 1.5$  cm, due to a vertical polarized normally incident plane wave, at the mid-point of the cylinder axis, for different strip widths.

The strip width is 0.045 cm. An array of  $10 \times 10$  elements is used with  $dz = 2.4$  cm and  $d\phi = 36^\circ$ . The radius of the cylindrical surface is 1.9 cm. A vertically polarized normally incident plane wave is incident on the structure. As shown in Figure 5, the stop band of the filter response is strongly dependent on the length of the strips, and the center of the band occurs approximately at a frequency where the length of the strip equals approximately half the wavelength of the incident plane wave. The effect of the width of the strip on the filter response of the cylindrical spatial filter is also investigated for different widths. As shown in Figure 6, the width of the strip has almost a negligible effect on the center frequency of the spatial filter, as the resonance characteristics of the strip is mainly a function of its length.

In the following results the strip dimension is fixed to length  $L = 1.5$  cm and width  $W = 0.045$  cm unless otherwise is stated.

### 3.1.3. Effect of Interelement Spacing on the Characteristics of the Cylindrical Spatial Filter

#### (a) Effect of Interelement Spacing in the $\phi$ -direction on the Filter Response

The effect of changing the circumferential spacing between the strips is investigated over the frequency range 5–15 GHz. This is done through increasing the number of elements in  $\phi$ -direction (i.e., decrease the spacing between the columns), while preserving the radius of the cylinder constant. The interelement spacing in the circumferential direction is studied for different number of columns, namely, 7, 10, 12, and 15 elements, corresponding to  $d\phi = 51.4^\circ, 36^\circ, 30^\circ,$  and  $24^\circ$ . In all cases, 10 elements in each column are used. The strip dimensions are  $1.5 \times 0.045$  cm. The radius of the cylinder is 1.9 cm, and the longitudinal spacing between the strips is  $dz = 2.4$  cm. The incident field is a vertically polarized plane wave propagating in the  $x$ -direction normal to the cylindrical surface. The transmitted field at the mid point of the cylinder axis is calculated and divided by the magnitude of the incident field to get the normalized frequency response of the spatial filter. As shown in Figure 7, increasing the circumferential spacing between the strips has the effect of reducing the center frequency and decreasing the bandwidth of the filter. This can be explained as follows. The coupling between elements increases as the interelement spacing decreases. This coupling causes the effective length of a strip to decrease, which in turns increases the resonant frequency. In Figure 8, the current distribution on the middle strip of the column of the array facing the incident wave is drawn, showing that the effective length on the strip (the length of the strip that has a significant current magnitude) decreases with decreasing the interelement spacing between the elements, which results in higher resonant frequency. This can be shown by taking

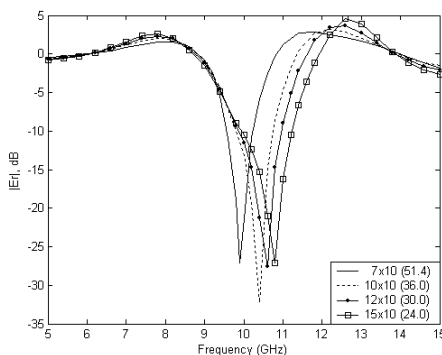


**Figure 7.** Frequency response of a cylindrical FSS with 10 elements in the longitudinal direction, the strip dimensions are  $1.5 \times 0.045$  cm,  $r = 1.9$  cm, and  $dz = 2.4$  cm, due to a normally incident plane wave with vertically polarized electric field, at the mid-point of the axis of the cylinder,  $|E_r| = |E_{Transmitted}|/|E_{incident}|$ .

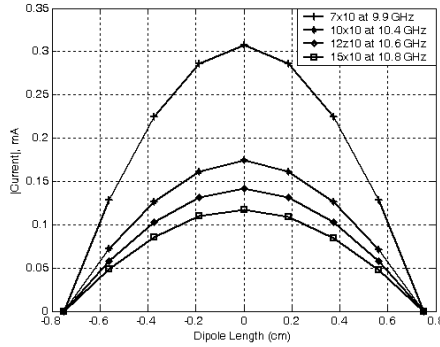


**Figure 8.** Current distribution at the center frequency of the stop band, on the middle strip of the column facing the incident wave.

the value 0.05 mA as a threshold above which the current magnitude is considered significant. It is clear that the  $15 \times 10$  array has the shortest effective length and the  $7 \times 10$  array has the longest effective length of the investigated arrays.

*(b) Effect of the Longitudinal Spacing on the Filter Response*

In the following results, the effect of changing the longitudinal (axial) spacing between the strips is investigated. The frequency response is studied for a normally incident plane wave with the electric field in the direction of the strips. The radius of the cylindrical surface is 1.9 cm. An array of  $10 \times 10$  elements is used with  $d\phi = 36^\circ$ . The longitudinal spacing between the strips in  $z$ -direction varies from 2 to 3.2 cm. The frequency response for different values of  $dz$  is shown in Figure 9. It can be seen from the figure that, increasing the interelement spacing will slightly decrease the bandwidth of the filter and slightly change the resonant frequency. This is because there exist a weak coupling between the elements in the axial direction even with decreasing the interelement spacing between them.

*3.1.4. Effect of Changing the Length of the Cylindrical Spatial Filter on Its Frequency Response*

The filter response of the cylindrical spatial filter is studied for different lengths of the cylindrical surface. The length of the cylindrical surface is designated by the number of elements in the longitudinal direction. Lengths of 5, 7, 10, and 15 elements are investigated, with 10 elements in the circumferential direction. The longitudinal spacing between the

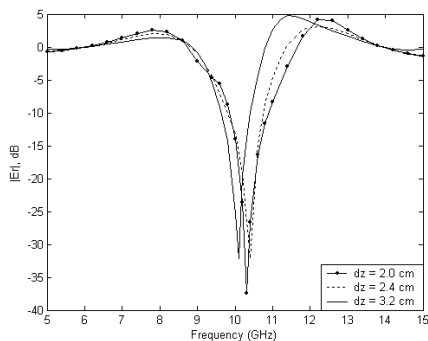


**Figure 9.** Frequency response of a cylindrical FSS composed of  $10 \times 10$  array with  $r = 1.9$  cm and  $d\phi = 36^\circ$ , due to a vertical polarized normally incident plane wave,  $|E_r| = |E_{Transmitted}|/|E_{incident}|$ .

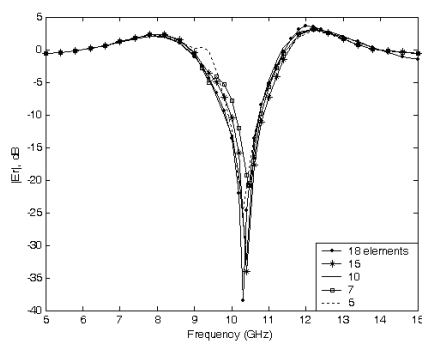


**Figure 10.** Filter response of a  $10 \times 10$  cylindrical FSS with various lengths, radius of cylinder  $r = 1.9$  cm,  $dz = 2.4$  cm, and  $d\phi = 36^\circ$ , the strip dimensions are  $1.5 \times 0.045$  cm.

strips  $dz$  is maintained at 2.4 cm, and the radius of cylindrical surface at 1.9 cm. It is clear from the results in Figure 10 that the length of the cylinder didn't affect much the center frequency of the band stop filter response, i.e., for the different lengths of the cylindrical spatial filter, the center frequency is located either at 10.3 or 10.4 GHz or in between them. It is also noted that the minimum of the frequency response curve decreases as the length of the cylinder increases.

### 3.1.5. Effect of Changing the Radius of the Cylindrical Spatial Filter on Its Frequency Response

The transmitted field at the center of the axis of a cylindrical spatial filter is calculated for different radii of the cylindrical surface, with a vertically polarized normally incident plane wave. The spatial filter is constructed up of  $10 \times 10$  strips, with longitudinal spacing between the strips  $dz = 2.4$  cm. The frequency response is obtained for different values of the radius  $r$ , 1.2, 2.4, and 3.2 cm. The circumferential distance between two adjacent dipoles is kept constant  $dr = 9.4$  mm. The excitation is a normally incident plane wave in the  $x$ -direction with the electric field in the  $z$ -direction. It can be seen from the results in Figure 11 that the radius of the cylinder has a profound effect on the frequency response of the spatial filter. It is responsible for determining the shape of the frequency response curve. There may

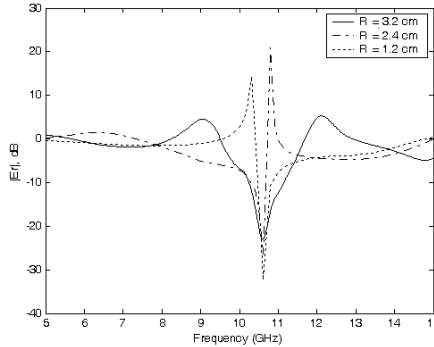


**Figure 11.** Frequency response of a cylindrical FSS with different radii,  $ds = 9.4$  mm, 10 elements in  $z$ -direction with  $dz = 2.4$  cm, the strip dimensions are  $1.5 \times 0.045$  cm, due to a vertically polarized  $x$ -directed normally incident plane wave.

appear some undesired peaks in the response that should be avoided. It is obvious from these results that, the radius of the cylindrical FSS is a very important parameter that should be determined before the other parameters, to guarantee that the FSS will not enhance the internal field to levels that could harm any enclosed object.

### 3.1.6. Oblique Incidence Effect on the Frequency Response of the Cylindrical Spatial Filter

The effect of the angle of incidence  $\theta$  (angle between the propagation vector and  $z$ -axis) on the frequency response of the cylindrical spatial filter is studied for different angles. The  $\phi$  angle (angle between the propagation vector and  $x$ -axis) is maintained at  $0^\circ$ , and the polarization angle  $\psi$  (angle between the projection of the electric field on the  $x$ - $y$  plane and  $x$ -axis) is also maintained  $0^\circ$ . A  $10 \times 10$  array is used with circumferential spacing between the strips  $d\phi = 36^\circ$  and longitudinal spacing between the strips  $dz = 2.4$  cm, and radius of 1.9 cm.  $\theta$  has changed from  $0^\circ$ – $90^\circ$ . Figures (12a)–(12d) shows the frequency response for different angles namely ( $30^\circ$ ,  $50^\circ$ ,  $70^\circ$ , and  $85^\circ$ ). It can be deduced from the figure that, not only the resonant frequency will changes, but also the whole frequency response curve may be deformed for certain range of  $\theta$ . The magnitude of the transmitted field will be maximized for some frequencies. In these cases, the cylindrical FSS will lose its filtering characteristics and can't be utilized as a spatial filter. From these results, it is concluded that the finite length cylindrical FSS will act as a spatial filter only for certain range of values

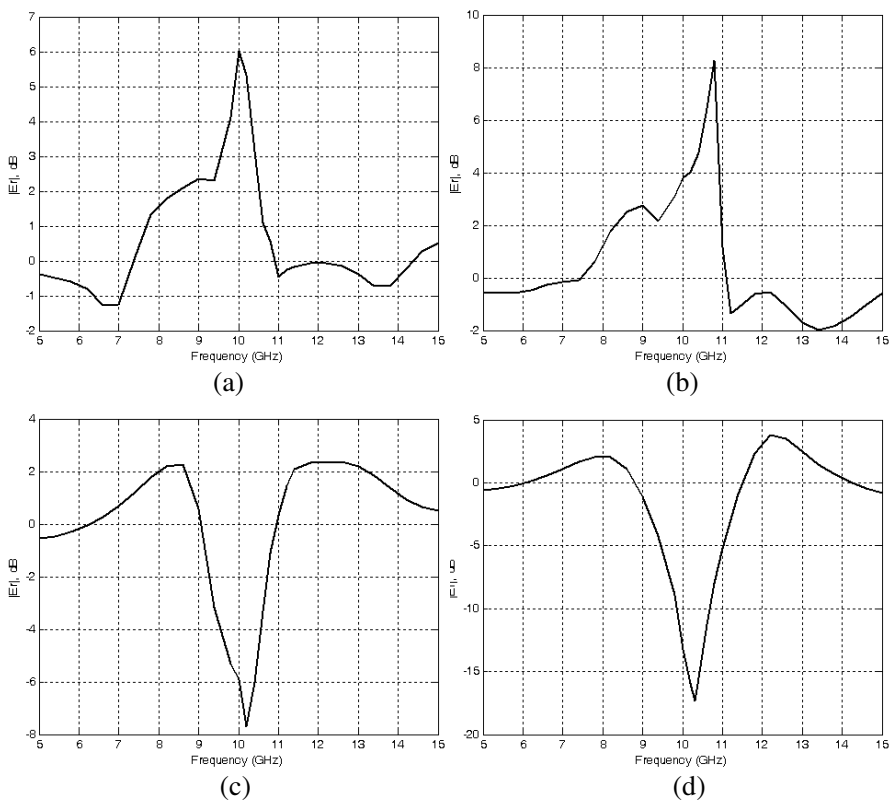


**Figure 12.** Frequency response for a  $10 \times 10$  cylindrical FSS with  $r = 1.9$  cm,  $d\phi = 36^\circ$ ,  $dz = 2.4$ , and strip dimensions  $1.5 \times 0.045$  cm cm for angles of incident (a)  $30^\circ$ , (b)  $50^\circ$ , (c)  $70^\circ$ , and (d)  $85^\circ$ .

for the angle  $\theta$ , namely from  $\approx 70^\circ$ – $110^\circ$ .

The effect of changing  $\phi$  is also studied for the same array. In this case,  $\theta = 90^\circ$  and  $\psi = 0^\circ$  and  $\phi$  changes from  $0^\circ$ – $360^\circ$ . The magnitude of the transmitted field at the mid point of the axis of the cylinder is studied at 10.4 GHz (the resonant frequency in Figure 2) for different values of  $\phi$ . As shown in Figure 13, the frequency response is almost independent of the  $\phi$  angle except for slight periodic changes of the magnitude of the field inside the cylindrical surface. It is also noted that the number of periods in Figure 13 equals the number of elements in the circumferential direction.

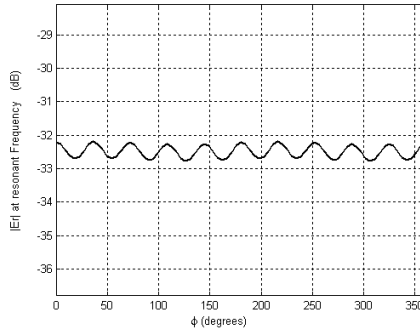


**Figure 13.** Frequency response for a  $10 \times 10$  cylindrical FSS with  $r = 1.9$  cm,  $d\phi = 36^\circ$ , and  $dz = 2.4$  cm, the strip dimensions are  $1.5 \times 0.045$  cm, due to a vertically polarized normally incident plane wave with  $\theta = 90^\circ$ ,  $\psi = 0^\circ$  and  $\phi$  changes from  $0^\circ$ – $360^\circ$ .

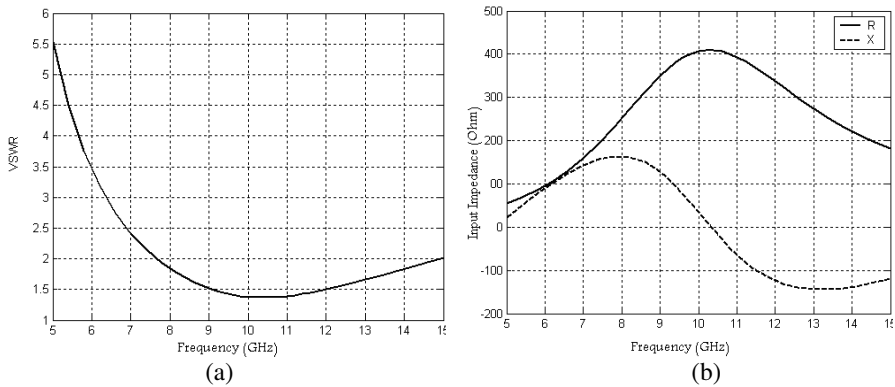


**Figure 14.** (a) VSWR. (b) Input impedance, against frequency of a Bowtie antenna in free space with length of 2.16 cm, flare angle  $45^\circ$ , neck width 1.08 mm excited with a delta gap voltage generator.

### 3.2. Frequency Response of a Bowtie Antenna Enclosed by Cylindrical Spatial Filter

A bowtie antenna is placed at the mid point of the axis of a  $12 \times 5$  cylindrical spatial filter, with  $r = 1.9$  cm,  $dz = 2.4$  cm, and  $d\phi = 30^\circ$ . The bowtie has a length of 2.16 cm with flare angle  $45^\circ$ . The neck width of the antenna (length of the excitation edge) is 1.08 mm. The bowtie is left to radiate in free space and excited with a delta gap voltage generator. The dependence of the VSWR and input impedance

of the bowtie is shown in Figure 14, where the source impedance is assumed  $300\ \Omega$ . Taking  $1 \leq \text{VSWR} \leq 1.5$  as a range for determining the bandwidth of the antenna, the bandwidth is about 3 GHz around the center frequency 10.5 GHz. Thus, this bowtie exhibit a relatively wide bandwidth, which will be a desired property to investigate the cylindrical spatial filter frequency response. The triangular-patch model of this antenna has 70 triangular patches and 89 non-boundary edges [19]. The frequency response of the free standing cylindrical spatial filter without the enclosed bowtie due to an  $x$ -directed vertically polarized plane wave propagating normal to the surface is shown in Figure 15.

### 3.2.1. Frequency Response of a Transmitting Bowtie Antenna

The bowtie of Section 3.2 is placed inside the cylindrical spatial filter with  $12 \times 5$  elements,  $r = 1.9$  cm,  $dz = 2.4$  cm, and  $d\phi = 30^\circ$ , the strip dimensions are  $1.5 \times 0.045$  cm, and excited by a delta gap voltage generator in the frequency band 5–15 GHz. The radiated field  $|E_\theta|$  is calculated at two locations, at a point 10 m away from the antenna along the  $x$ -axis, and at a point 10 m along the  $y$ -axis.

The normalized radiated field is also calculated for a bowtie in free space without the spatial filter at the same locations and plotted in Figure 16. Figure 17 shows the frequency response of the bowtie antenna (normalized radiated field with the cylindrical FSS present divided by the normalized radiated field without FSS) at the two

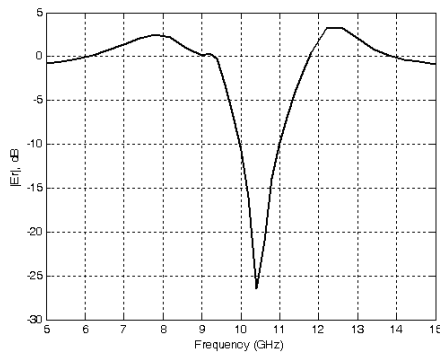


**Figure 15.** Frequency response of the free standing  $12 \times 5$  cylindrical FSS, with  $r = 1.9$  cm,  $dz = 2.4$  cm, and  $d\phi = 30^\circ$ , strip dimensions are  $1.5 \times 0.045$  cm, excited by a vertically polarized  $x$ -directed normally incident plane wave.

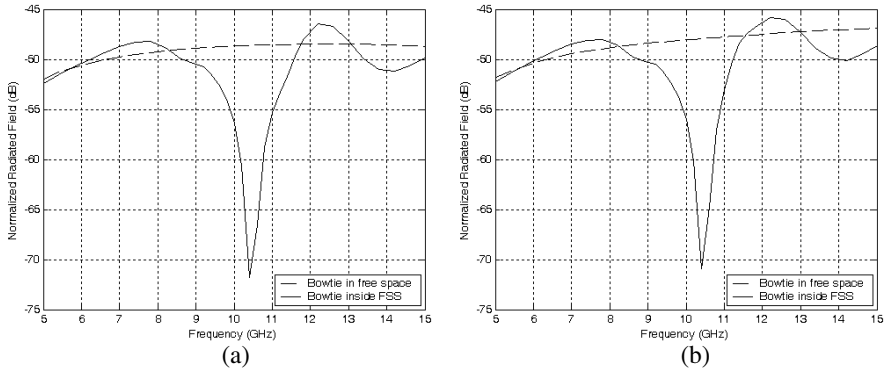


**Figure 16.** Normalized radiated field from the bowtie antenna of length = 2.16 cm, Neck width = 1.08 mm, and flare angle =  $45^\circ$ , at a point 10 m along the (a)  $x$ -axis, (b)  $y$ -axis.

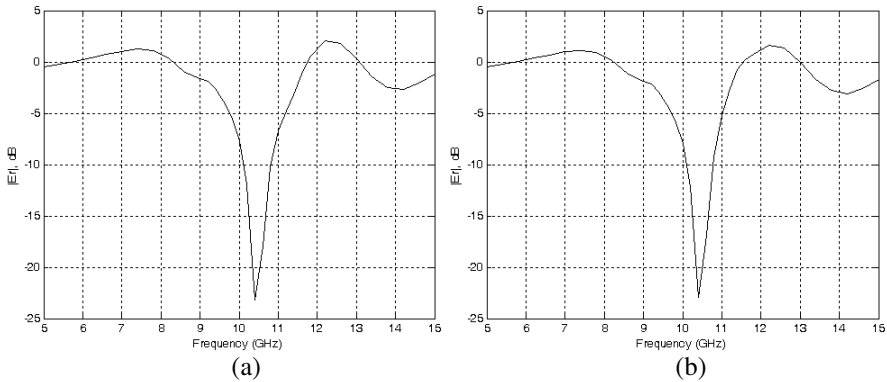


**Figure 17.** Frequency response of the bowtie antenna at a point 10 m along (a)  $x$ -axis, (b)  $y$ -axis.

locations. It is obvious from Figure 15 and Figure 17, that the center frequency of the FSS and the band width have not been changed due to the presence of the antenna.

### 3.2.2. Frequency Response of a Receiving Bowtie Antenna

The bowtie of Section 3.2 is enclosed by the  $12 \times 5$  cylindrical spatial filter, with  $r = 1.9$  cm,  $dz = 2.4$  cm, and  $d\phi = 30^\circ$ , strip dimensions are  $1.5 \times 0.045$  cm, and used as a receiver. A plane wave is incident on the structure in  $x$ -direction with the electric field in  $z$ -direction

with amplitude of 1 V/m. The received voltage is calculated in the frequency range 5–15 GHz for the bowtie inside the FSS and in free space as shown in Figure 18(a). The received voltage is calculated as  $I_{in}Z_{in}$ , where  $Z_{in}$  is the input impedance and  $I_{in}$  is the induced current

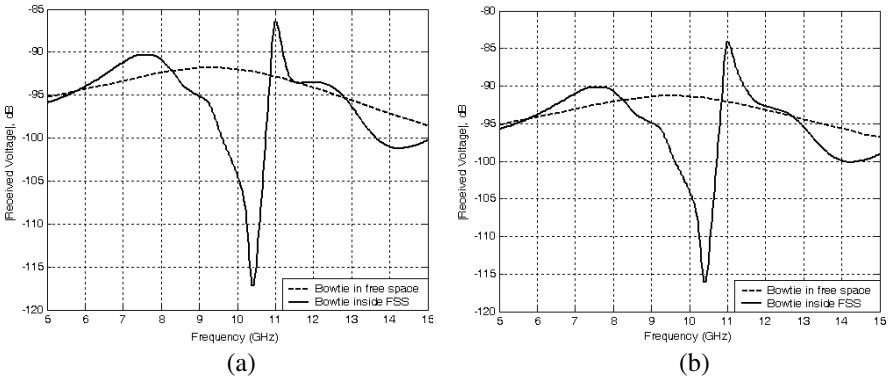


**Figure 18.** Received voltage by a bowtie antenna with length = 2.16 cm, Neck width = 1.08 mm and flare angle = 45°, enclosed inside a 12 × 5 cylindrical FSS with,  $r = 1.9$  cm,  $dz = 2.4$  cm, and  $d\phi = 30^\circ$ , strip dimensions are 1.5 × 0.045 cm, due to an incident plane wave in (a)  $x$ -direction, (b)  $y$ -direction, with  $z$ -directed electric field (1 V/m).

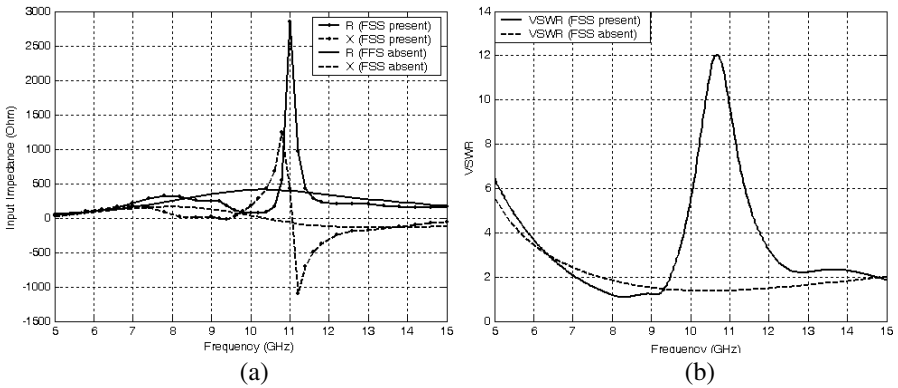


**Figure 19.** Comparison between input impedance and VSWR of a bowtie antenna in free space and in the presence of a 12 × 5 cylindrical spatial filter FSS with  $r = 1.9$  cm,  $dz = 2.4$  cm, and  $d\phi = 30^\circ$ , strip dimensions are 1.5 × 0.045 cm, Bowtie Length = 21.6 mm, Neck width = 1.08 mm and Flare angle = 45°. (a) Input impedance, (b) VSWR.

at the excitation edge. Figure 18(b) shows the received voltages when the incident wave is a  $y$ -directed normally incident plane wave. It is clear that the FSS has spatially filtered the incident field within its stop band.

### 3.2.3. Effect of the Cylindrical Spatial Filter on the Input Impedance of the Enclosed Antenna

The effect of a  $12 \times 5$  cylindrical spatial filter with  $r = 1.9$  cm,  $dz = 2.4$  cm, and  $d\phi = 30^\circ$ , strip dimensions are  $1.5 \times 0.045$  cm, on

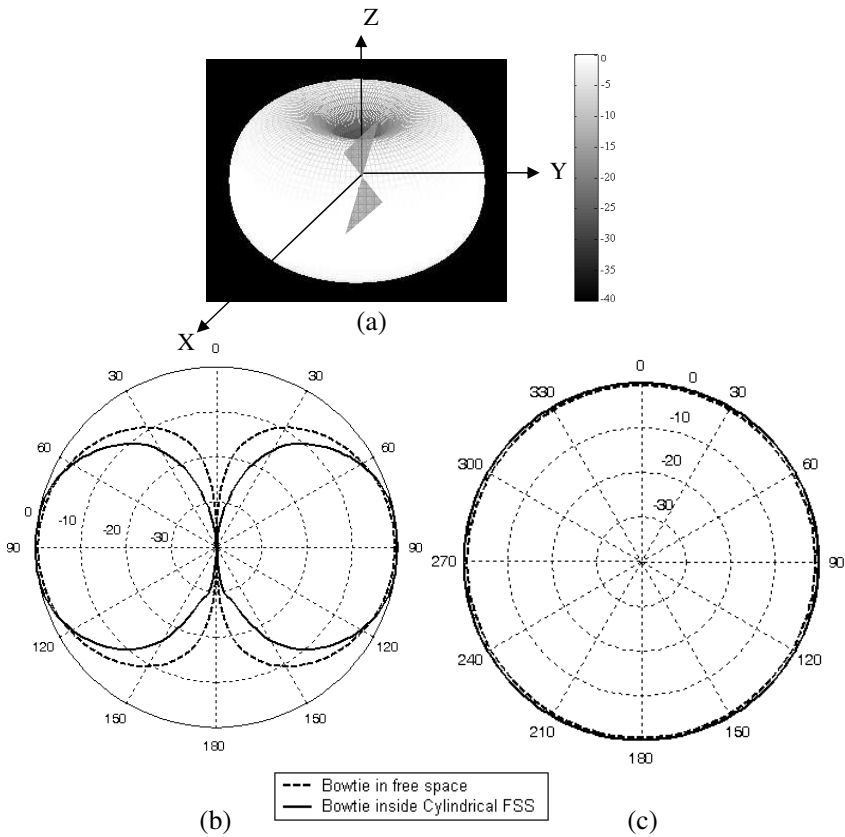


**Figure 20.** Radiation pattern for a bowtie antenna (Length = 21.6 mm, Neck width = 1.08 mm and Flare angle =  $45^\circ$ ) placed on the axis of the  $12 \times 5$  Cylindrical FSS ( $r = 1.9$  cm,  $dz = 2.4$  cm, and  $d\phi = 30^\circ$ , strip dimensions are  $1.5 \times 0.045$  cm), at  $f = 7.8$  GHz, (a) 3D plot, (b) Elevation plane  $\phi = 90^\circ$ , (c) Azimuth plane  $\theta = 90^\circ$ .

the input impedance and VSWR of a bowtie antenna similar to that used in Section 3.2, placed at the center of the axis of the filter cavity is investigated in the frequency range 5–15 GHz. Figure 19(a) shows the real and imaginary parts of the input impedance of the bowtie when placed at the center of the axis of the cylindrical spatial filter compared to its input impedance when radiating in free space. In

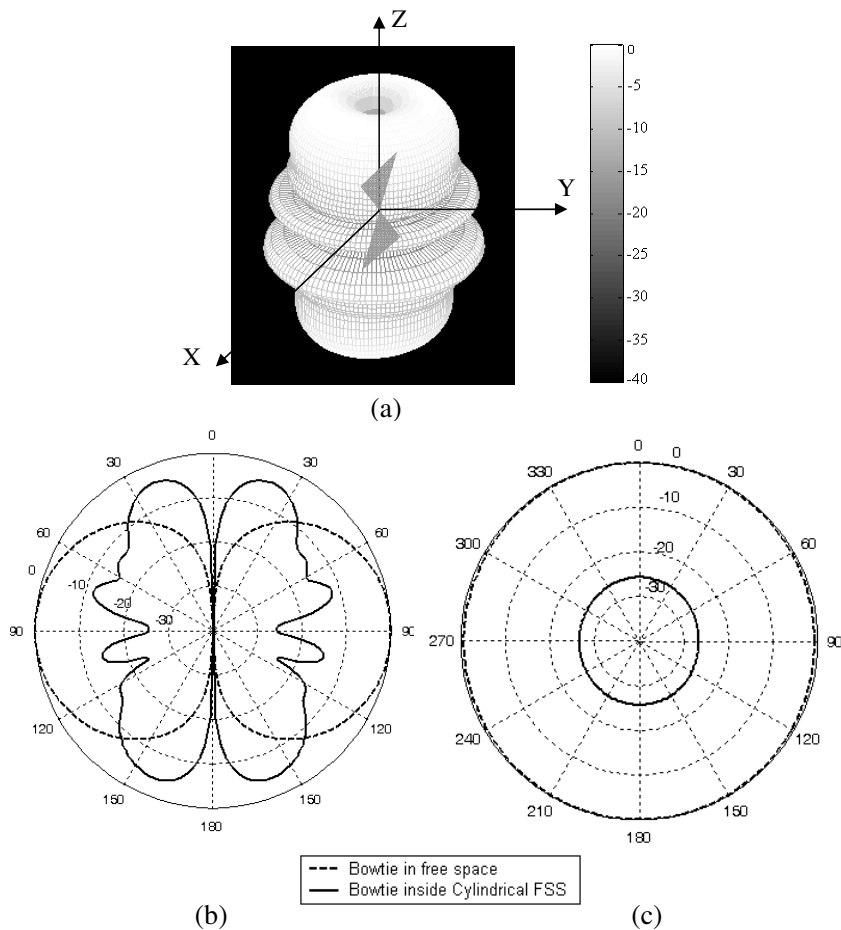


**Figure 21.** Radiation pattern for a bowtie antenna (Length = 21.6 mm, Neck width = 1.08 mm and Flare angle = 45°) placed on the axis of the 12 × 5 Cylindrical FSS ( $r = 1.9$  cm,  $dz = 2.4$  cm, and  $d\phi = 30^\circ$ , strip dimensions are  $1.5 \times 0.045$  cm), at  $f = 10.4$  GHz, (a) 3D plot, (b) Elevation plane  $\phi = 90^\circ$ , (c) Azimuth plane  $\theta = 90^\circ$ .

Figure 19(b), the VSWR of the bowtie is calculated and compared to that of an antenna placed in free space over the frequency range 5–15 GHz. Although VSWR shows bad antenna performance within the stop band of the filter, one shouldn't care about this, as the function of the cylindrical spatial filter is to prevent the antenna transmission and reception within the stop band.

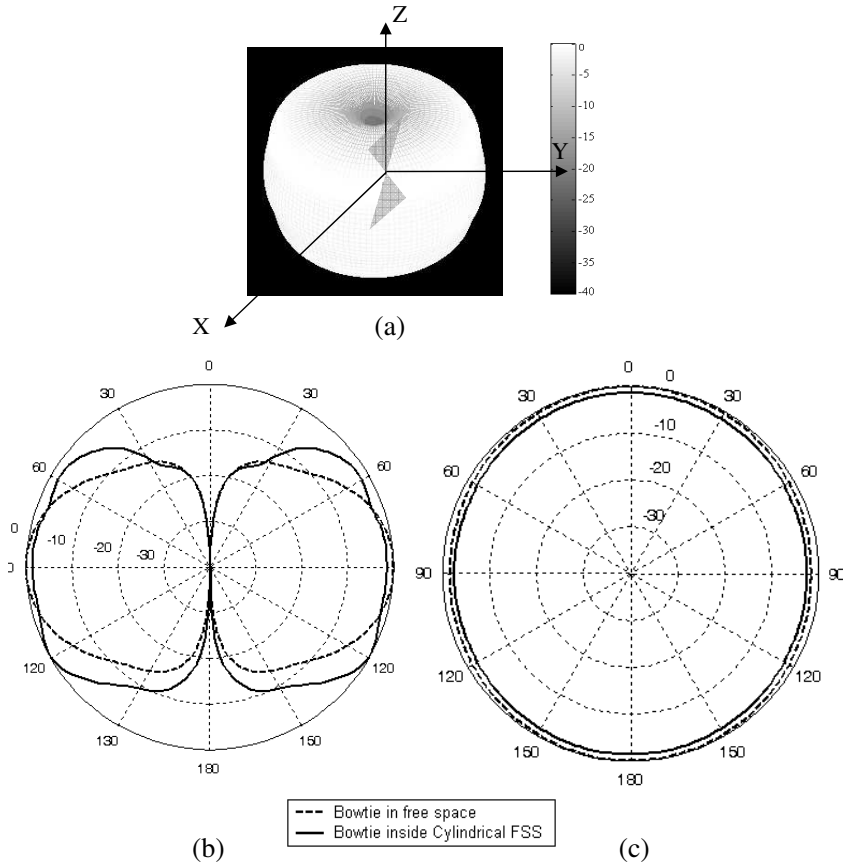


**Figure 22.** Radiation pattern for a bowtie antenna (Length = 21.6 mm, Neck width = 1.08 mm and Flare angle =  $45^\circ$ ) placed on the axis of the  $12 \times 5$  Cylindrical FSS ( $r = 1.9$  cm,  $dz = 2.4$  cm, and  $d\phi = 30^\circ$ , strip dimensions are  $1.5 \times 0.045$  cm), at  $f = 14.2$  GHz, (a) 3D plot, (b) Elevation plane  $\phi = 90^\circ$ , (c) Azimuth plane  $\theta = 90^\circ$ .

### *3.2.4. Effect of the Cylindrical FSS on the Radiation Patterns of the Enclosed Antenna*

The effect of the cylindrical spatial filter on the radiation pattern of the enclosed bowtie is studied at different frequencies. The testing frequencies are 7.8 GHz (frequency before the stop band), 10.4 GHz (center of the stop band) and 14.2 GHz (frequency after the stop band). The radiation patterns in the elevation and the azimuth planes are shown in Figures 20–22. The radiation patterns are compared to that of the antenna in free space (without the spatial filter). It is noticed from the figures that the far field is diminished at the center frequency of the stop band (10.4 GHz), and that the radiation intensity is considerably reduced between ( $40^\circ < \theta < 140^\circ$ ). Also, the radiation intensity has been increased between ( $0^\circ < \theta < 40^\circ$ ). As shown in Figures 20 and 22 the cylindrical spatial filter has almost no bad effect on the radiation pattern of the enclosed antenna at the frequencies outside the stop band of the filter. It is also noticeable in all the cases, that the radiation pattern of the bowtie antenna inside the cylindrical spatial filter is still omnidirectional in the azimuth plane. In conclusion, one can abstract that a cylindrical spatial filter like that proposed in the present work has the basic advantages of diminishing the radiation from the enclosed antenna at frequencies within the stop band while keeping the radiation properties at the other frequencies especially the omnidirectionality in the azimuth plane.

## **4. CONCLUSION**

In this paper, the EFIE is used to study the frequency response of a cylindrical frequency selective surface, constructed up of an array of strips. It is found that the proposed FSS has a band stop filter response. The center frequency of this band is equal to the resonant frequency of the constructing strips. The effect of some dimensional parameters on the filter response is investigated in the frequency range 5–15 GHz. It is found that increasing the interelement spacing in  $\phi$ -direction will decrease the bandwidth of the spatial filter and will alter the center frequency, but increasing the interelement spacing in  $z$ -direction has a negligible effect on the frequency response. The length of the cylinder is found decrease the minimum of the frequency response curve as the length increase. The radius was found to have a profound effect on the filter response, as it controls the shape of the frequency response curve. Changing the angle of incidence has a great effect on the filtering characteristics of the cylindrical spatial filter. For a range of  $\theta$  the cylindrical structure will increase the internal fields. That is there is only a reasonable range of  $\theta$  where the cylindrical structure

will act as a spatial filter. The angle  $\phi$  was found to have a negligible effect on the FSS filter response.

A bowtie antenna is enclosed by the cylindrical spatial filter, and the normalized radiated field is obtained in the frequency range 5–15 GHz. The effect of the spatial filter on the bowtie input impedance and VSWR is studied in the same frequency band. It is found that the presence of the cylindrical FSS has spoiled the antenna performance within the stop band which is desired. Also the effect of the spatial filter on the radiation pattern of the enclosed bowtie antenna is investigated at different frequencies. It is noticed that the cylindrical FSS has not changed the omnidirectionality of the antenna and didn't affect the radiation pattern outside the stop band. The bowtie is also used as a receiver. The received voltage is calculated when a vertically polarized normally incident plane wave is incident on the structure. It is found that the FSS will filter the signal within its stop band.

## REFERENCES

1. Cwik, T., R. Mittra, K. C. Lang, and T. K. Wu, "Frequency selective screens," *IEEE Antennas Propagat. Soc. Newsletter*, 6–10, Apr. 1987.
2. Agrawal, V. D. and W. A. Imbriale, "Design of dichroic cassegrain subreflector," *IEEE Antennas Propagat. Trans.*, Vol. 27, No. 6, 466–473, Jul. 1979.
3. Gerini, G. and L. Zappelli, "Multilayer array antennas with integrated frequency selective surfaces conformal to a circular cylindrical surface," *IEEE Antennas Propagat. Trans.*, Vol. 53, No. 6, Jun. 2005.
4. Sung, G. H., K. W. Sowerby, M. J. Neve, and A. G. Williamson, "A frequency-selective wall for interference reduction in wireless indoor environments," *IEEE Antennas Propagat Magazine*, Vol. 48, No. 5, Oct. 2006.
5. Lalezari, F. and P. A. Zidek, "Antenna system utilizing frequency selective surface," US Patent No. 5982339, Nov. 1999.
6. Wu, T. K., J. J. Macek, and Bever, "Frequency selective surface filter for an antenna," US Patent No. 5949387, Sep. 1999.
7. Qing, A., "Vector spectral-domain method for the analysis of frequency selective surfaces," *Progress In Electromagnetics Research*, Vol. 65, 201–232, 2006.
8. Vardaxoglou, J. C., *Frequency Selective Surface, Analysis and Design*, Research Studies Press Ltd., Taunton, England, 1997.
9. Chen, C. C., "Scattering by a two dimensional periodic array of

- conducting plates,” *IEEE Trans. Antennas Propagat.*, Vol. 18, 660–665, 1970.
10. Alexopoulos, N. G., P. L. E. Uslenghi, and N. K. Uzunoglu, “Microstrip dipoles on cylindrical structures,” *1981 Antennas Applications Symposium Proceedings*, University of Illinois, Sep. 1981.
  11. Cwik, T., “Coupling into and scattering from cylindrical structure covered periodically with metallic patches,” *IEEE Trans. Antennas Propagat.*, Vol. 38, No. 2, 220–226, Feb. 1990.
  12. Uzer, A. and T. Ege, “Radiation from a current filament located inside a cylindrical frequency selective surface,” *ETRI Journal*, Vol. 26, No. 5, 481–485, Oct. 2004.
  13. Cwik, T. and R. Mittra, “The effects of truncation and curvature of periodic surfaces: A strip grating,” *IEEE Trans. Antennas and Propagat.*, Vol. 36, 612–622, May 1988.
  14. Carogalnian, A. and K. J. Webb, “Study of curved and planar frequency-selective surfaces with non-planar illumination,” *IEEE Trans. Antennas Propagat.*, Vol. 39, No. 2, 211–217, Feb. 1991.
  15. Ko, W. L. and R. Mittra, “Scattering from an array of metallic patches located on a curved surface,” *IEEE Antennas Propagat. Soc. Dig.*, 642–645, Syracuse, NY, 1988.
  16. Rao, S. M., D. R. Wilton, and A. W. Glisson, “Electromagnetic scattering by surfaces of arbitrary shape,” *IEEE Trans. Antennas Propagat.*, Vol. 30, 409–418, May 1982.
  17. Hussein, K. A., “Fast computational algorithm for EFIE applied to arbitrarily shaped conducting surface,” *Progress In Electromagnetics Research*, Vol. 68, 339–357, 2007.
  18. Farahat, A. E., K. A. Hussein, and N. M. El-Minyawi, “Spatial filters for linearly polarized antennas using free standing frequency selective surface,” *Progress In Electromagnetics Research M*, Vol. 2, 167–188, 2008.
  19. Hussein, K. A., “Efficient near field computation for radiation and scattering from conducting surfaces of arbitrary shape,” *Progress In Electromagnetics Research M*, Vol. 69, 267–285, 2007.
  20. Hussein, K. F. A., “Accurate computational algorithm for calculation of input impedance of antennas of arbitrary shaped conducting surfaces,” *ACES*, Vol. 22, No. 3, Nov. 2007.